Coalescence of droplets due to a constant force interaction in a quiescent viscous fluid

John M. Frostad, Alexandra Paul, and L. Gary Leal

Phys. Rev. Fluids **1**, 033904 — Published 25 July 2016

DOI: 10.1103/PhysRevFluids.1.033904

Coalescence of Droplets Due to a Constant Force Interaction in a Quiescent, Viscous Fluid

John Frostad[a]*, Alexandra Paul[a,b], Gary Leal[a]
[a] Department of Chemical Engineering, University of California, Santa Barbara 93106 (United States of America)
[b] Department of Biophysical Chemistry, Saarland University, Saarbrucken 66123 (Germany)
**Corresponding author: frostad@engineering.ucsb.edu*

Abstract
A cantilevered-capillary force apparatus is used to study the time scale for the coalescence of two droplets compressed together with a constant force. Power-law trends for the coalescence time as a function of droplet radius and compression force are experimentally measured. The measurements are compared against several different scaling theories from the literature. One of the existing theories is found to correctly predict the dependence on the droplet radius, but all of the theories over-predict the dependence on the force. A transition is also observed in the measured drainage time from a having a small variation around a single deterministic value for droplets with a radius of 125 μm or less, to a broad distribution of drainage times for droplets with a radius of 150 μm. A qualitative explanation for this transition is provided via scaling arguments.

1. Introduction
Many everyday items such as shampoo, mayonnaise, and beauty crèmes are emulsions. The quality of these products is tied to the tendency of the emulsions to phase separate over time. A fundamental understanding of the phase separation process, via coalescence in particular, will enable improved processing of these products and better product quality. In many of these products, the emulsion droplets are very small and therefore their behavior can often be modeled in the viscous flow (low Reynolds number) regime. Numerous experimental and theoretical studies of coalescence in viscous systems have been performed over the last 50 years to understand this process. Reviews by Chesters [1], Leal [2], and Janssen and Anderson [3] provide a detailed summary of much of this work.

Despite the extensive work that has been done, the coalescence process is a very complicated one and the dynamics of even simplified systems involving only two droplets, lack a unifying theoretical description. This is not to say that the two-droplet interaction cannot be successfully modeled numerically. Various groups have used numerical methods to study the complete flow field for droplets colliding and coalescing in a flow [3,4,5]. There has also been extensive work on numerically modeling a simplified system based upon the thin-film approximation [6,7,8,9,10,11,12,13]. However, a change in the system configuration or system parameters (such as droplet radius or viscosity) requires that the numerical model, whether based on the full problem or the thin-film approximation, be solved again for the new conditions. Therefore, simpler, scaling-type descriptions involving the system parameters would be more useful

from the point of view of developing design equations for the commercial production of emulsions. For example, the time scale over which two colliding droplets must interact before they will coalesce is important for determining emulsion stability. Many scaling relations have been proposed over the years to predict the time scale for coalescence [14], but each new model tends to reveal insight that invalidates or conflicts with previous models. The various assumptions built into these models also tend to be difficult to validate experimentally making it difficult to know which model (if any) is accurate.

Of primary importance in establishing a fundamental understanding, is designing experiments that provide a good testing ground for theoretical ideas. Because of the broad interest in this field, many different experimental techniques exist that study simplified systems with this purpose in mind. Noteworthy examples include coalescence between droplets held on capillaries observed with laser interferometry [15], thin film studies in a Sheludko-type cell [16], buoyancy driven coalescence [17,18], flow induced coalescence in a 4-roll mill device [4,19], and in a modified atomic force microscope (AFM) [20]. In this work, a new instrument called a Cantilevered-Capillary Force Apparatus (CCFA) [21] is used to measure the time required for coalescence of two, 100 – 250 μm sized droplets in a quiescent fluid. The only other experimental data on coalescence time that is similar to the data collected in the present work was collected using a modified AFM [12,13,20], but those data sets are rather limited for testing scaling predictions and are not directly comparable because the fluids used were much less viscous and the time scales for coalescence were three orders of magnitude smaller than in the present study.

In the CCFA, the droplets are held on the tips of two opposing capillaries as shown in Figure 1. One advantage of using this technique is that the force of interaction can be precisely controlled and/or measured during the collision as explained in section 2. Another advantage of this experimental setup is that the conditions for coalescence are qualitatively similar to the phase separation process that determines the shelf-life of an emulsified product. While "on the shelf," freely suspended droplets interact through a constant force due to buoyancy (provided that they are large enough to overcome thermal motion). The magnitude of this force depends on the size of the droplets, the density difference between the two fluids, and the orientation of the interaction relative to gravity.

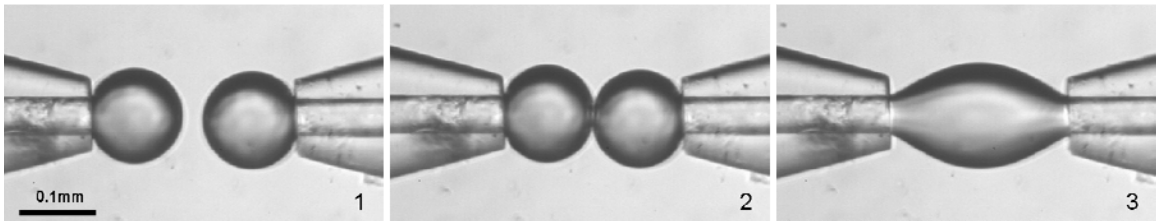

Figure 1. Image of two droplets held by capillaries in an axisymmetric configuration (1). The droplets can be pressed together with a constant force (2) until they coalesce (3).

Because the CCFA is a new technique, a portion of the materials and methods section is devoted to describing how it functions during a typical experiment. This includes a brief description of a buckling-type instability that limits the maximum force that can be applied between the droplets. In addition to studying coalescence, it is also possible to

measure the interfacial tension of the system under study as described in section 3.1. Sections 3.2 and 3.3 are used to present existing theoretical predictions from the literature and compare them to measurements of the drainage time performed in the CCFA. In the process of making the drainage time measurements it was also observed that the distribution of measured drainage times becomes surprisingly large for the largest droplets studied. The observation and a possible explanation are discussed in section 3.4.

2. Materials and Methods

2.1. Instrument and Fluid System

A schematic representation of the CCFA is shown in Figure 2 and a full description of the instrument can be found in a previous paper [21]. Briefly, the CCFA consists of two capillaries in which one of the capillaries acts as a force transducer. The capillary that acts as a force transducer is bent to a 90° angle and has a mirror attached near the end. A laser is reflected off of the mirror to monitor the deflection of the cantilever with a typical resolution of ~10 nm in this study. The time resolution of the measured deflection can be adjusted within the range allowed by the data acquisition card used (National Instruments USB-6009) and was set to 100 Hz for all measurements in this study. This results in an uncertainty of ± 0.01 s for each time measurement. The spring constant of the cantilever depends on the length, which changed slightly whenever the apparatus was dismantled for cleaning (about once per week). In each case, the spring constant was carefully calibrated and for the majority of the data presented in this paper was 46.8 ± 0.9 mN/m.

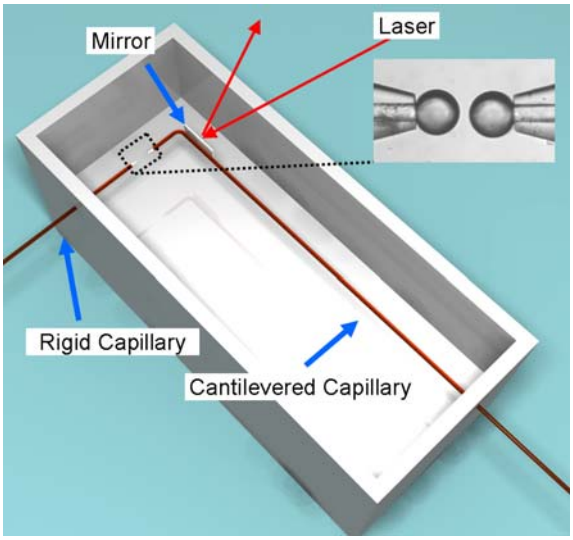

Figure 2. Schematic representation of the Cantilever-Capillary Force Apparatus (CCFA).

The second capillary (referred to as the "rigid capillary") is able to move forward and backward at controlled velocities ranging between 0.1 – 600 μm/s. The position of the rigid capillary is controlled with a resolution of a few nanometers when moving in a single direction and a repeatability of ~1 μm when reversing directions. The relatively poor repeatability when reversing directions is a consequence of a small amount of play in the mechanical connection between the positioning stage and the metal arm holding

the rigid capillary. Both capillaries can be submerged in a liquid (suspending fluid) inside the device, and are connected to reservoirs of the fluid used to supply the droplet fluid.

A comparison of the CCFA to similar instruments, including advantages of using the CCFA for the present experiments can also be found in a previous paper [21]. Briefly, the process of creating and positioning droplets for interaction in the CCFA is trivial in contrast to devices such as the AFM and the Integrated Thin Film Drainage Apparatus (ITFDA) [22]. In the CCFA it is possible to easily produce two equal-sized droplets with a radius from ~10 μm to greater than 200 μm, within 1 μm of the desired size (the measurement error is estimated to be ≤ 300 nm). In addition, the spring constant can be measured with ~1 – 2% uncertainty, compared with 10 – 20% in an AFM and around 20% in the ITFDA. Finally, the droplets are pinned to the edges of the capillary so that the contact angle is free to change, which is important for producing similarity to two freely suspended droplets. Producing droplets with pinned contact lines for two droplets should be straight forward in the ITFDA (though attempts to do so have not been published), but in an AFM it requires careful, chemical functionalization of circular patches on the cantilever and opposing substrate.

In this study, 1000 cS polydimethylsiloxane (PDMS, $\rho =$ 971 kg/m^3, *UCT Specialties*) is used as the droplet fluid to generate two "equal" size droplets with a radius between 50 – 125 μm, at the tips of the capillaries. As noted above, the size of each droplet is matched so that they are equal to within 1 μm. An effective radius is then computed as $R = \frac{2R_1R_2}{R_1 + R_2}$ [7], which corresponds to the radius which produces the average capillary pressure of the two droplets. The same two capillaries were used for all coalescence experiments and they had an inner diameter of 50 ± 3 μm (*New Objective TT150-50-50-N-5*). The CCFA chamber was filled with 650 cP polybutadiene (PBD, $\rho = 900$ kg/m^3, 1,530 – 2,070 M_n, *Sigma Aldrich*) as the suspending fluid. The interfacial tension of the system was measured using both the pendant drop method, and the CCFA to be ~4 mN/m. The temperature in the laboratory was maintained at approximately 22°C for all experiments.

Coalesced droplets were removed from the tips of the capillaries by gently stirring the chamber fluid, and fresh droplets of PDMS were pushed out of the capillaries using hydrostatic pressure for each coalescence experiment. Before every experiment it is ensured that the volume of the droplets is constant with time by adjusting the hydrostatic pressure while monitoring the growth rate. The growth rate is monitored via real-time analysis in Matlab of images taken through an optical microscope.

2.2. Constant Force Interaction

To produce a constant force interaction between two droplets, it would be possible to use feedback control to maintain a set force, but this adds unnecessary complexity to the interaction and experimental procedure. Instead, a simpler way to achieve an approximately constant force interaction is used in the present experiments. Here the rigid capillary is simply moved forward a certain distance until the droplets are under compression and then held at that position until coalescence takes place. Before moving

the droplets together, they are held stationary with the center-to-center distance equal to 2.5 times the droplet radius. From this initial separation an experiment to measure the drainage time is started. Data from a typical experiment are shown in Figure 3a to illustrate the procedure.

As indicated by the dashed line in Figure 3a, the rigid capillary is moved forward at a constant velocity until the droplets are pressed together and held at this position until coalescence is observed. Some discussion is required regarding the transient force measured as the droplets are being moved together (from ~3 seconds to ~10 seconds in Figure 3a). The relatively high viscosity of the suspending fluid causes the drag force acting on the cantilever, due to the motion of the rigid capillary, to be significant. This drag force results in a much larger deflection of the capillary than what would be caused by the interaction of the droplets alone.

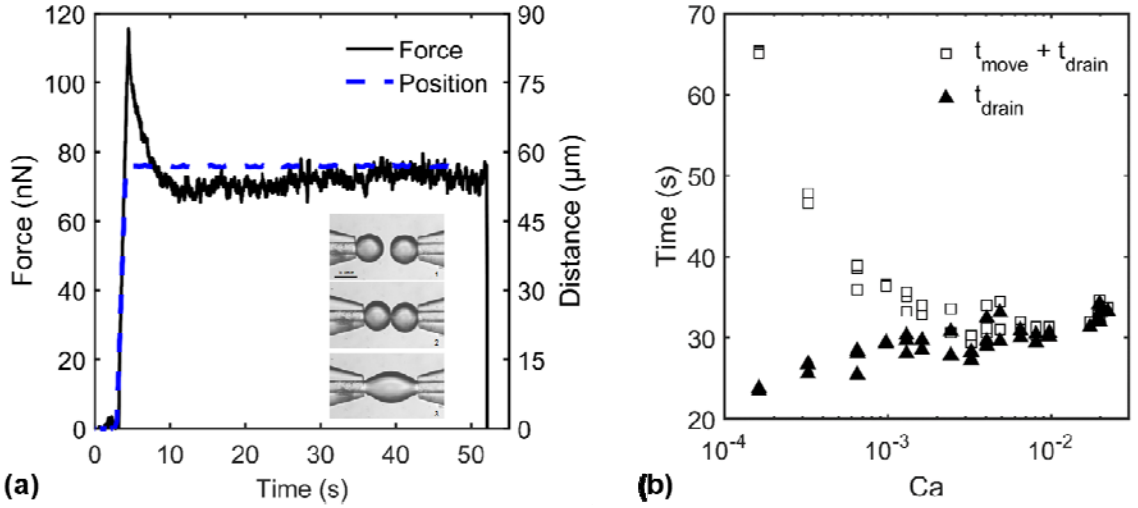

Figure 3 (a) Typical force curve for a constant force interaction. The dashed blue line shows the position of the rigid capillary (right y-axis). The black line shows the force as a function of time (left y-axis). The sharp downturn in the force curve at around 52 s signals coalescence. (b) Drainage time as a function of the capillary number (1 – 136 μm/s) for $\overline{F} = 0.31 \pm 0.06$ (R_{eq} = 75 μm; $F = 94 \pm 17$ nN). Note than the open symbols correspond to the full experiment time including the initial approach period, while the solid symbols are the actual drainage times.

Fortunately, this additional drag force and the magnitude of the approach velocity have minimal impact on the drainage time. Bazhlekov et al. [23] found in numerical simulations that above a minimum velocity, increasing the velocity further has negligible impact on the drainage of the film and that the initial constant velocity portion of the collision is "without influence" on the ultimate drainage. To confirm that this is the case, the drainage time was measured as a function of the velocity of the rigid capillary for a given droplet size and applied force. For evaluating the results, the operating parameters (velocity, force, and radius) are nondimensionalized, resulting in a capillary number Ca and a dimensionless force parameter $\overline{F}$:

$$Ca \equiv \frac{\mu V}{\gamma}; \qquad \overline{F} \equiv \frac{F}{\gamma R}. \tag{1}$$

Here μ is the viscosity of the suspending fluid, V is the velocity of the rigid capillary, γ is the interfacial tension, F is the magnitude of the applied force when it becomes constant with time, and R is the initial radius of the undeformed droplets. The dimensionless force parameter can be thought of as a generalization of the capillary number.

The drainage time t_{drain} in this paper is defined as starting from the time the rigid capillary stops moving (at ~4.5 seconds in Figure 3a) until coalescence occurs. Coalescence is signaled in the measurements by a rapid decrease in the measured force, seen at ~52 seconds in Figure 3a. As predicted by Bazhelkov et al. [23], Figure 3b shows that with increasing velocity, the drainage time (solid symbols) becomes essentially independent of approach velocity. In this case, for $\overline{F} = 0.31 \pm 0.06$, the drainage time stops increasing when the value of the capillary number exceeds about 10^{-3} (> 6 μm/s). This is also consistent with the experimental results of Zdravkov et al. [24].

The drainage time could be defined in other ways. For example, in previous work from our group, the drainage time was defined as beginning from the instant when the center-to-center separation of the two droplets is equal to twice their undeformed radius. This condition is physically meaningful because if the droplets were non-deforming, that is exactly the point at which they would touch (coalesce), resulting in $t_{\text{drain}} = 0$. However, as shown by the open symbols in Figure 3b, at larger velocities the time spent while the capillary is moving t_{move} (starting at ~3 s in Figure 3a), becomes insignificant compared to the drainage time. This means that any refinement in the convention for setting t=0, to include all or part of t_{move}, would produce a very small change in the reported drainage times.

Because of the relative insensitivity of the drainage time to the approach velocity, there is some flexibility in choosing the velocity for the experiments. In the present study, the velocity was selected such that the capillary number associated with the initial motion was proportional to $\overline{F}$ so that the deformation of the droplets induced by motion will be proportional to the deformation due to the statically applied force. In all cases, the velocity was high enough that Ca > 10^{-3} and in the most extreme case for the data collected in this study, $t_{\text{move}} = 5.12$ s when $t_{\text{drain}} = 27.66$ s.

A final point of consideration is the assumption of an axisymmetric geometry in the development of the theory and interpretation of the measurements of drainage time. The axisymmetric orientation of the droplets and capillaries depends on the axisymmetry of the capillaries and their alignment, but also on the force applied to the droplets. It is observed that when the droplets are compressed beyond a certain point they spontaneously "slide" out of axisymmetry as depicted in Figure 4. Initially the droplets are stable to non-axisymmetric perturbations until a critical compression is reached (Figure 4b). Above this critical compression the axisymmetric configuration becomes

unstable and the droplets will adopt a non-axisymmetric configuration (Figure 4c) [25]. In order to preserve the axisymmetry of the experiments, care was taken to apply only forces small enough that this instability did not occur.

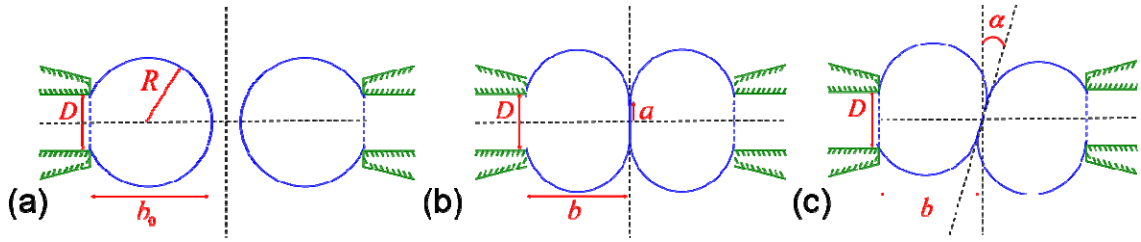

Figure 4. Depiction of two droplets held by capillaries interacting under a compressive force. (a) Before contact. (b) Under symmetric compression. (c) After the critical force is reached and a non-axisymmetric configuration is more stable.

3. Results and Discussion

3.1. Interfacial Tension

For performing and interpreting measurements of the drainage time it is important to know the interfacial tension of the fluid-fluid system. One of the advantages of using the CCFA for these measurements is that the interfacial tension can easily be determined by measuring the force required to stretch a single droplet held between the tips of the capillaries as shown in Figure 5a. The stretching force can be related to the interfacial tension by the well-established theory of capillary bridges (see, for example, the text by Myshkis et al [26]). The exact solution of the Young-Laplace equation for a droplet between two capillaries was derived by Howe (translated and repeated by Gillette and Dyson [27,28]), which yields analytical formulae for the force on the capillaries (albeit in terms of unwieldy parameters). Recently, Kusumaatmaja and Lipowsky [29] gave a linear approximation to the force exerted by a liquid bridge, valid for small deformations from equilibrium ($F = 0$), repeated here for reference (equation (45) in [29]):

$$\frac{k}{\gamma} = \frac{-\pi}{\ln(\csc\theta + \cot\theta) - \frac{\cos\theta}{1+\cos^2\theta}}. \qquad (2)$$

Here k is the effective spring constant of the droplet and θ is the equilibrium contact angle of the droplets defined as follows, assuming that $R > D/2$:

$$\theta = \frac{\pi}{2} + \arccos\left(\frac{D}{2R}\right). \qquad (3)$$

Equations (2) and (3) provide an explicit analytical formula that is very convenient for measuring the interfacial tension. The results of stretching one droplet of radius R are plotted in Figure 5a where the reference length L_0 corresponds to the equilibrium distance between the capillaries when the force is zero. Here the sign convention is taken such that a repulsive force is positive and an attractive force is negative. The slope of the linear portion of the curve in Figure 5a at small perturbations from L_0 was taken as the experimental value of the effective spring constant of the droplet. The effective spring

constant was measured as a function of the radius of the droplet R divided by the mean diameter D of the two capillaries (D_1 and D_2) for a range of droplet radii and compared to the prediction from equation (2). The value of the interfacial tension measured by solving the Young-Laplace equation for the full stretching curve in Figure 5a (solid line) with the interfacial tension as a fitting parameter was 3.94 mN/m. Using this value of the surface tension directly in equation (2), Figure 5b shows good agreement between the measured, effective spring constant and the theoretically predicted value (without any additional fitting) for a wide range of droplet sizes. Given that each data point corresponds to a new droplet it can be concluded that the value of the interfacial tension is very consistent from one experiment to the next.

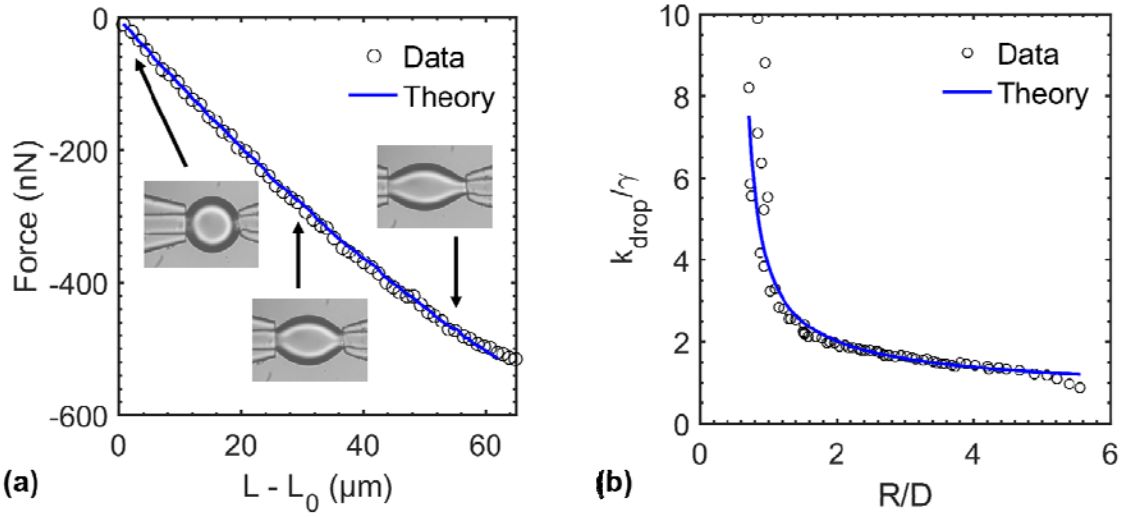

Figure 5. (a) Force as a function of the stretched distance for a droplet of PDMS in PBD ($R = 71.1$ μm; $D_1 = 62$ μm; $D_2 = 55$ μm). The interfacial tension from fitting the data is 3.94 mN/m. (b) Effective spring constant of the droplet divided by the measured interfacial tension as a function of the droplet radius divided by the capillary diameter.

3.2. Prediction(s) of Drainage Time

As described in the introduction, numerous researchers over the last 50 years have worked on this problem. Because of this, several theoretical predictions exist that provide a scaling relationship for the drainage time as a function of droplet radius and interaction force. Unfortunately, none of these predictions for the drainage time has yet been convincingly validated by comparison with numerical simulations or experimental results. The more popular among these models are based upon writing an expression for the drainage rate of suspending fluid out of the film separating the droplets. The film is expected to drain and grow thinner until a critical film thickness h_c is reached at which point Van der Waals forces act to quickly rupture the film according to the following scaling [30,31,32]:

$$\frac{h_c}{R} \sim \bar{F}^{1/6} A^{1/3}. \qquad (4)$$

Here $\bar{F}$ and A are the dimensionless force and dimensionless Hamaker constant defined along with the dimensionless drainage time τ as follows:

$$\tau = \frac{t_d \gamma}{\mu R}; \qquad \overline{F} = \frac{F}{\gamma R}; \qquad A = \frac{A_H}{\gamma R^2}. \tag{5}$$

Here t_d is the drainage time, γ is the interfacial tension, R is the undeformed droplet radius, F is the applied force on the droplets (assumed to be constant), and A_H is the Hamaker constant. For this system A_H has a value of 3.6×10^{-21} J.

Using the criterion for the critical film thickness in equation (4) along with a few prominent thin film drainage models from the literature, the experimental data can be compared to the respective predictions. A very early model derived by several different authors [17,33] is still widely used in the literature. Chesters presented a review of this model applied to droplets with both tangentially mobile and immobile interfaces (numbers 1 and 2 in Table 1) [1]. The key assumptions built into these early models are that the thin film between the droplets is of uniform thickness and that the pressure gradient in the radial direction is constant across the film. It has been acknowledged that the assumption of uniform thickness [33] is not strictly physical because the thin film is known to be thinnest at the outer edge of the film, due to the formation of a dimple in the droplets near the center of the film. Recently, Frostad et al. (2013) made an observation regarding the pressure gradient driving the drainage of the thin film that extends the model to account for this non-uniform thickness [34]. One of the advantages to the model developed in [34] is that it directly accounts for the transition from a uniform film to a dimpled film. The analysis of Frostad et al. is partially repeated here to illustrate how the drainage models are used to predict the drainage time.

All of the models mentioned in the previous paragraph begin with a rate equation for the thickness of the film such as that given by Frostad et al. [34]:

$$\frac{dh}{dt} \sim -\frac{uh}{a}. \tag{6}$$

Here h is the minimum film thickness (with respect to position), t is time, u is the average velocity of the fluid in the thin film at the location of the minimum film thickness, and a is the radial extent of the thin film. By balancing the force applied on the droplets with the force due to the capillary pressure multiplied by the thin film area, the radial extent of the thin film is found to scale as:

$$a \sim R\overline{F}^{1/2}. \tag{7}$$

The scaling for the velocity in the film depends on the mobility of the interface. In the absence of Marangoni effects due to surface active compounds, or other mechanisms that would inhibit motion of the droplet interfaces, the effective mobility depends on the viscosity ratio according to:

$$u \sim u_p\left(1 + k\frac{l_c}{\lambda h}\right) \qquad \lambda \geq O(1). \tag{8}$$

Here u_p is the pressure driven component of the velocity, k is an $O(1)$ constant, and l_c is the length scale over which the pressure varies from the value in the center of the film to the value in the bulk fluid. According to the analysis of Frostad et al. l_c scales as

$l_c \sim \sqrt{hR}$, while in previous models it is assumed to scale as $l_c \sim a$. For very large values of the viscosity ratio or in the presence of a sufficient concentration of surface active compounds (which may either lead to Marangoni stresses or significant interfacial viscosities), the droplet interfaces are essentially immobile. In that case, the velocity in the film scales with the pressure driven component of the velocity u_p:

$$u_p \sim \frac{\gamma h^2}{\mu R l_c}. \tag{9}$$

On the other hand, equation (8) shows that when $\lambda \sim O(1)$ and the interfaces are mobile, the scaling of the velocity changes because $h/l_c << 1$ [34].

For the case when the interfaces are immobile, substituting equations (7) and (9) into (6) and integrating yields:

$$\frac{R}{h_c} - \frac{R}{h_0} \sim \frac{\gamma}{\lambda \mu R \overline{F}^{1/2}} t_d. \tag{10}$$

Assuming that the critical film thickness h_c at which rupture occurs is much smaller than the initial film thickness h_0 and using equation (4), the result is:

$$t_d \sim F^{1/4} R^{7/4} \left[\mu \gamma^{-3/4} A_H^{-1/2} \right], \tag{11}$$

or in dimensionless terms:

$$\tau \sim \overline{F}^{1/4} A^{-1/2}. \tag{12}$$

This is listed as prediction number 5 in Table 1. The same procedure outlined in equations (6) - (12) can be followed using the alternate scaling for l_c, ($l_c \sim a$) to arrive at the prediction of the earlier model (listed in Table 1 as prediction number 1). On the other hand, when the interfaces are mobile such that the thin film velocity is predominantly of the plug-flow type, the length scale of the pressure gradient l_c drops out. In this case, because the scaling for l_c does not influence the model, the prediction of Frostad et al. and earlier models give the same result (number 2 in Table 1).

In addition to the these basic thin film models, a few authors have made predictions for the scaling behavior of the drainage time based on numerical models including the detailed shape of the thin film. Nemer et al. (2006) use an asymptotic approach to predict the rate of film thinning for mobile interfaces at very long times [35]:

$$\overline{h}_m \sim \overline{\tau}^{-4/3}; \qquad \overline{h}_m \equiv \frac{hR}{a^2}; \qquad \overline{\tau} \equiv \frac{t\gamma a}{2\mu R^2}. \tag{13}$$

Converting to the same dimensionless variables used in this paper gives the prediction listed as number 3 in Table 1. Chen et al. (1984) developed a model for a non-uniformly thinning film that includes the effect of Van der Waals forces on the drainage process for immobile interfaces [36]. Their prediction is listed as number 4 in Table 1 for the case when the Van der Waals force is non retarded ($m = 3$ in their paper, where m is the exponent for the distance dependence of the disjoining pressure). Still other predictions can be found in the literature, but the selected set is a reasonable representation of the variety that exist. In the next subsection experimental results are presented for comparison.

Table 1. Various predictions from the literature for the scaling behavior of the drainage time.

Source	Non-Dimensional	Dimensional
1. Charles & Mason (1960) [17]	$\tau \sim \overline{F}^{2/3} A^{2/3}$	$t_d \sim R^{5/3} F^{2/3} \approx R^{1.67} F^{0.67}$
2. Chesters (1991) [1]	$\tau \sim \lambda \overline{F}^{1/3} A^{-1/3}$	$t_d \sim R^{4/3} F^{1/3} \approx R^{1.33} F^{0.33}$
3. Nemer et al. (2006) [35]	$\tau \sim \lambda \overline{F}^{13/24} A^{-5/12}$	$t_d \sim R^{31/24} F^{13/24} \approx R^{1.29} F^{0.54}$
4. Chen et al. (1984) [36]	$\tau \sim \overline{F}^{1/2} A^{-1/2}$	$t_d \sim R^{3/2} F^{1/2} = R^{1.5} F^{0.5}$
5. Frostad et al. (2013) [34]	$\tau \sim \overline{F}^{1/4} A^{-1/2}$	$t_d \sim R^{7/4} F^{1/4} = R^{1.75} F^{0.25}$
Experimental Data	-	$t_d \sim R^{1.78\pm0.1} F^{0.053\pm0.035}$

3.3. Experimental Drainage Time Data

The dependence of the drainage time on the droplet radius and applied force was studied in the CCFA by varying the force while holding the radius constant, and varying the radius while holding the force constant. As mentioned in the introduction, all experiments were performed such that the capillary number corresponding to the initial constant velocity motion to bring the droplets together exceeded 10^{-3} and is proportional to the dimensionless force. The measurements show that the drainage time increases very slightly with increasing force, but increases much more strongly with increasing radius. The data can be reduced to a scaling relationship by fitting the data to a power-law as shown in Figure 6:

$$t_d \sim R^{1.78\pm0.1} F^{0.053\pm0.035}. \quad (14)$$

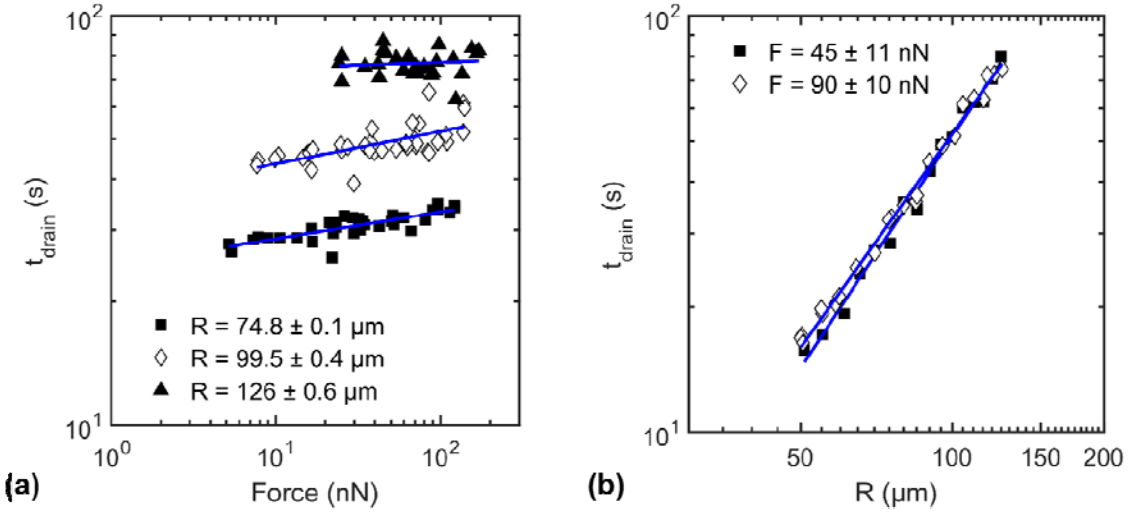

Figure 6. Drainage time as a function of applied force (a) and droplet radius (b). The symbols represent the data and the solid lines represent a power-law fit to the data with slopes and 95% confidence intervals of (a) 0.066 ± 0.016, 0.079 ± 0.032, and 0.014 ± 0.048 with respect to increasing radius and (b) 1.85 ± 0.14 and 1.71 ± 0.08 with

increasing force.

Comparing the data to the theoretical predictions in Table 1 a couple of observations can be made. First, all of the models predict a dependence on the applied force that is stronger than what is observed experimentally. The authors were not able to resolve this discrepancy in the present work, but this trend is suggestive of a common problem in the models. Although the authors can only speculate on the source(s) of the problem, one suggestion is that the condition for rupture of the film (due to Van der Waals forces) is critical to producing the correct prediction and merits further consideration. Another observation is that models that are based on immobile interfaces (numbers 1, 4 and 5 in Table 1) tend to have a stronger dependence on the droplet radius than the models with mobile interfaces (numbers 2 and 3 in Table 1).

Given that the data exhibit a strong dependence on the droplet radius, this would suggest that the present system may contain surface active contaminants that immobilize the interface. It was believed initially that there should be no surface active compounds present in this system, but it is very difficult to guard against trace amounts of contamination. In general it is difficult to find a system of two immiscible fluids that are known to be completely free from surface active contaminants. Needing to anticipate the effect of unknown surface active compounds makes it even more difficult to establish a working model for predicting drainage time.

Of the models that were reviewed for this study, the model of Frostad et al. gives the best agreement with the data in that the dependence of the radius matches the data and that it predicts the weakest dependence on the applied force. This is somewhat encouraging, but it is clear that further work is needed. It is worth reiterating that the experimental data collected in this study confirm that power-law relations *can* be used to describe/predict the time scale for coalescence, which further motivates additional theoretical effort.

3.4. Stochasticity of Drainage Time

An interesting complexity of the coalescence process is that while thin film drainage is a deterministic process, the rupture of the film is due to an instability which is inherently stochastic [32]. The total drainage time measured in an experiment therefore depends on both of these processes. The variability of the drainage time Δt_{drain} that is measured will depend on the distribution of times (or film thicknesses) accessible to the rupture mechanism of the film relative to the total drainage time t_{drain}. If the magnitude of the variability in the stochastic process is much smaller than the drainage time $\Delta t_{\text{drain}} << t_{\text{drain}}$ then any observed variability in the measurement can be attributed to experimental error. On the other hand if the variability in the stochastic process is of the same order of magnitude as the drainage time then variability will be observed in the measurements that is larger than what could be attributed to experimental error. Such behavior was qualitatively observed in the course of the present work and similar unreported measurements of the drainage time. To partially quantify this observation, the distribution of drainage times measured for 50 experiments each, at three values of the droplet radius

are shown in Figure 7. In each case the applied force was the same within experimental error at ~105 nN.

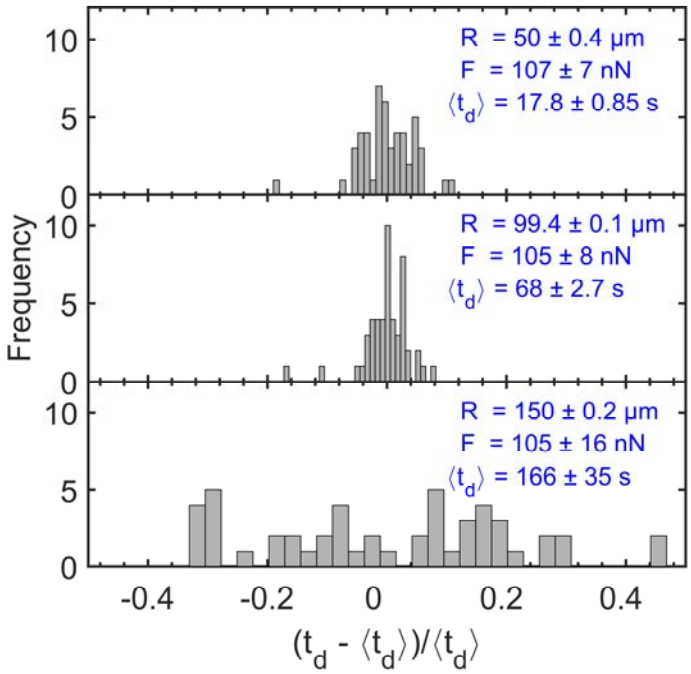

Figure 7. Histogram showing the distribution of drainage times at R = 50, 100, 150 μm for 50 repeated measurements at the same applied force and velocity. Inset to each plot is a summary of the mean values and standard deviations of the droplet radius, applied force, and measured drainage times from all 50 measurements in each case.

For droplets with a radius of around 50 and 100 microns, the variability in the drainage time measurements are approximately the same with a variation of ~5 - 10%. This similarity in the level of variation suggests that is it largely experimental error due to small systematic differences from one experiment to the next, such as small differences in the droplet radii, applied force, or alignment of the capillaries. For droplets with a radius of 150 microns however, the variability is quite large and the distribution is comparatively flat over a wide range for the same number of measurements. This larger variability is further accentuated by the fact that the time drainage time is the longest of the three cases and the time spent moving the droplets together is only 0.98 seconds compared to the average drainage time of 166 seconds. This suggests that the variability in the stochastic process has become comparable to the total drainage time. In other words, it is possible that for larger droplets, the time required for the film to drain to the critical film thickness in a deterministic fashion may be prematurely shortened by random finite amplitude perturbations in the film. Such finite amplitude perturbations are possible due to simple environmental vibration even when using a vibration damping table. The question then is how much of the drainage process is cut short due to a perturbation of a given magnitude.

This question can be partly addressed by an appeal to the models presented in subsection 3.2. Equation (6) for the rate of change of the film thickness as a function of time can be rewritten for the critical thickness h_c at which rupture occurs using equation (4) as:

$$\frac{dh}{dt} \sim -\frac{\gamma}{\mu}\left(\frac{h_c}{R}\right)^{5/2} \overline{F}^{-1/2} \qquad \rightarrow \qquad \frac{dh}{dt} \sim -\frac{\gamma}{\mu} A^{5/6} \overline{F}^{-1/12}. \tag{15}$$

This equation can then be inverted to give the rate of change in the drainage time with respect to changes in the critical film thickness:

$$\left|\frac{dt_d}{dh}\right| \sim \frac{\mu}{\gamma}\left(\frac{A_H}{\gamma R^2}\right)^{-5/6}\left(\frac{F}{\gamma R}\right)^{1/12} \qquad \rightarrow \qquad \left|\frac{dt_d}{dh}\right| \sim R^{19/12} \approx R^{1.58}. \tag{16}$$

It is clear from this relation that the length of time by which the drainage time can be shortened due to a finite perturbation of the film thickness of a given magnitude dh, increases with the radius of the droplets. This is consistent with the observations and provides a qualitative explanation. For the purposes of comparing the deterministic part of the theory to measured drainage time, large droplet radii were avoided in the data presented in the previous subsection to avoid further complication to the interpretation.

It can be seen however that for the largest droplets in Figure 6 that a slightly increased variation in the data is observed. At much larger droplet radii such as those in the early experiments of Charles and Mason [17] and others, the drainage time is found to be a stochastic quantity where distributions rather than values of the drainage time are measured. The present findings therefore suggest that there is a physical mechanism to explain why measured drainage times would appear to be deterministic in one study, but stochastic in another.

4. Conclusion

Drainage time data were collected for the coalescence of two droplets pressed together with a force that is approximately constant with time. Data for droplets with a radius smaller than 125 μm are consistent with a deterministic process leading to film rupture, and were found to display power-law relationships between the drainage time and the experimentally varied parameters: droplet radius and interaction force. Data for the largest droplet size studied (150 μm radius) showed a high degree of variability, qualitatively consistent with a stochastic process leading to film rupture. A qualitative explanation for why this high level of variability should appear for larger droplets was offered based on a thin film drainage model.

The experimentally measured scaling of the drainage time for the deterministic cases was compared to several predictions from the literature, but none of these models showed complete quantitative agreement. A common shortcoming in all of the models was identified, namely that the predicted dependence on the applied force is too strong in every case. In addition, all models except for that by Frostad et al. [34] predict a dependence on the droplet radius that is too weak. Nevertheless, the fact that the experiments demonstrate clear power-law trends, shows that further work is needed to advance theoretical models to the point of successfully predicting the time scale of coalescence.

5. Acknowledgements

This work was supported by the Institute for Multi-scale Materials Studies at Los Alamos National Laboratory and the National Science Foundation. Alexandra Paul was partially supported by the CISEI internship program through the Institute for New Materials, Saarland University, the UCSB Materials Research Laboratory and the International Center for Materials Research under grants NSF DMR 1121053 and NSF DMR 08-43934.

The authors would like to gratefully acknowledge Professor Gwynn Elfring for helpful discussions regarding the instability at large compression forces and for reviewing an earlier version of this manuscript.

6. References

1. A.K. Chesters, "The Modeling of Coalescence Processes in Fluid Liquid Dispersions - A Review of Current Understanding," Chemical Engineering Research & Design **69**, 259 (1991).
2. L.G. Leal, "Flow induced coalescence of drops in a viscous fluid," Physics of Fluids **16**, 1833 (2004).
3. P.J.A. Janssen and P.D. Anderson, "Modeling Film Drainage and Coalescence of Drops in a Viscous Fluid," Macromolecular Materials and Engineering **296**, 238 (2011).
4. Y. Yoon, F. Baldessari, H.D. Ceniceros, and L.G. Leal, "Coalescence of two equal-sized deformable drops in an axisymmetric flow," Physics of Fluids **19,** 102102-1 (2007).
5. B. Dai and L.G. Leal, "The mechanism of surfactant effects on drop coalescence", Physics of Fluids, **20,** 040802 (2008).
6. S.G. Yiantsios and R.H. Davis, "Close appraoch and deformation of two viscous drops due to gravity and van der Waals forces", J. Colloid Interface Sci **144**, 412 (1991).
7. R.H. Davis, J.A. Schonberg, and J.M. Rallison. "The Lubrication Force between Two Viscous Drops," Physics of Fluids A: Fluid Dynamics 1, 77 (1989).
8. M.A. Rother, A.Z. Zinchenko and R.H. Davis, "Buoyancy-driven coalescence of slightly deformable drops", J. Fluid Mech. **346**, 117 (1997).
9. S.G. Yiantsios and R.H. Davis, "On the buoyancy driven motion of a drop towards a rigid surface or a deformable interface", J. Fluid Mech. **217**, 547 (1990).
10. F. Baldessari and L.G. Leal, "Effect of overall drop deformation on flow-induced coalescence at low capillary numbers", Physics of Fluids, **18,** 103602 (2006).
11. M.B. Nemer, P. Santioro, X. Chen J. Blawzdziewicz and M. Loewenberg, "Coalescence of drops with mobile interfaces n a quiescent fluid", J. Fluid Mech. **728,** 471 (2013).
12. Vakarelski, Ivan U., Rogerio Manica, Xiaosong Tang, Sean J. O'Shea, Geoffrey W. Stevens, Franz Grieser, Raymond R. Dagastine, and Derek Y. C. Chan. "Dynamic Interactions between Microbubbles in Water." *Proceedings of the National Academy of Sciences* 107, no. 25 (June 22, 2010): 11177–82. doi:10.1073/pnas.1005937107.
13. Manica, Rogério, Jason N. Connor, Raymond R. Dagastine, Steven L. Carnie, Roger G. Horn, and Derek Y. C. Chan. "Hydrodynamic Forces Involving

Deformable Interfaces at Nanometer Separations." *Physics of Fluids (1994-Present)* 20, no. 3 (March 1, 2008): 032101. doi:10.1063/1.2839577.
14. Y. Liao and D. Lucas, "A literature review on mechanisms and models for the coalescence process of fluid particles," Chemical Engineering Science **65**, 2851 (2010).
15. E. Klaseboer, J. Chevaillier, C. Gourdon, and O. Masbernat, "Film drainage between colliding drops at constant approach velocity: Experiments and modeling," Journal of Colloid and Interface Science **229**, 274 (2000).
16. L.G. Cascao Pereira, C. Johansson, H.W. Blanch, and C.J. Radke, "A bike-wheel microcell for measurement of thin-film forces," Colloids and Surfaces A: Physicochemical and Engineering Aspects **186**, 103 (2001).
17. G.E. Charles and S.G. Mason, "The coalescence of liquid drops with flat liquid/liquid interfaces," Journal of Colloid Science **15**, 236 (1960).
18. M. Manga and H.A. Stone, "Buoyancy-Driven Interactions Between Two Deformable Viscous Drops," Journal of Fluid Mechanics **256**, 647 (1993).
19. H. Yang, C. Park, Y. Hu, and L. Leal, "The coalescence of two equal-sized drops in a two-dimensional linear flow," Physics of Fluids **13**, 1087 (2001).
20. H.J. Lockie, R. Manica, G.W. Stevens, F. Grieser, D.Y.C. Chan, and R.R. Dagastine, "Precision AFM Measurements of Dynamic Interactions between Deformable Drops in Aqueous Surfactant and Surfactant-Free Solutions," Langmuir **27**, 2676 (2011).
21. J.M. Frostad, M.C. Collins, and L.G. Leal, "Cantilevered-Capillary Force Apparatus for Measuring Multiphase Fluid Interactions," Langmuir **29**, 4715 (2013).
22. L. Wang, D. Sharp, J. Masliyah, and Z. Xu. "Measurement of Interactions between Solid Particles, Liquid Droplets, and/or Gas Bubbles in a Liquid Using an Integrated Thin Film Drainage Apparatus." Langmuir **29,** 3594 (2013).
23. I.B. Bazhlekov, A.K. Chesters, and F.N. van de Vosse, "The effect of the dispersed to continuous-phase viscosity ratio on film drainage between interacting drops," International Journal of Multiphase Flow **26**, 445 (2000).
24. A. Zdravkov, G.W. Peters, and H.E. Meijer, "Film drainage between two captive drops: PEO–water in silicon oil," Journal of Colloid and Interface Science **266**, 195 (2003).
25. G.J. Elfring and E. Lauga, "Buckling instability of squeezed droplets," Physics of Fluids **24**, 072102 (2012).
26. A.D. Myshkis, V.G. Babskii, N.D. Kopachevskii, L.A. Slobozhanin, and A.D. Tyuptsov, "Low-Gravity Fluid Mechanics: Mathematical Theory of Capillary Phenomena," (Springer, 2011).
27. W. Howe, Die Rotations-Flächen, Ph.D. Thesis, Universität zu Berlin, Germany (1887).
28. R.D. Gillette and D.C. Dyson, "Stability of fluid interfaces of revolution between equal solid circular plates," Chemical Engineering Journal **2**, 44 (1971).
29. H. Kusumaatmaja and R. Lipowsky, "Equilibrium Morphologies and Effective Spring Constants of Capillary Bridges," Langmuir **26**, 18734 (2010).

30. A. Vrij and J. Th. G. Overbeek. “Rupture of Thin Liquid Films due to Spontaneous Fluctuations in Thickness,” Journal of the American Chemical Society **90**, 3074 (1968).
31. R.J. Gumerman, J. Raymond, and G.M. Homsy. “The Stability of Radially Bounded Thin Films,” Chemical Engineering Communications **2**, (1975).
32. S. Kaur and L.G. Leal, “Three-dimensional stability of a thin film between two approaching drops,” Physics of Fluids **21**, 072101 (2009).
33. D. Chappelear, “Models of a liquid drop approaching an interface,” Journal of Colloid Science **16**, 186 (1961).
34. J.M. Frostad, J. Walter, and L.G. Leal, “A Scaling Relation for the Capillary-Pressure Driven Drainage of Thin Films,” Physics of Fluids **25**, 052108 (2013).
35. M.B. Nemer, X. Chen, D.H. Papadopoulos, J. Bławzdziewicz, and M. Loewenberg, “Comment on ‘Two touching spherical drops in uniaxial extensional flow: analytic solution to the creeping flow problem’,” Journal of Colloid and Interface Science **308**, 1 (2007).
36. J.-D. Chen, P.S. Hahn, and J.C. Slattery, “Coalescence time for a small drop or bubble at a fluid-fluid interface,” AIChE Journal **30**, 622 (1984).